Optimal Reaching Method for Enhanced Higher-Order Sliding Mode Control of Electro-Hydraulic Servo Systems

Peng Wan , Yunfei Wang * , Jiawen Yang

Posted Date: 17 September 2025

doi: 10.20944/preprints202509.1471.v1

Keywords: asymmetric cylinder; electro-hydraulic system; high-order sliding mode control; optimal reaching

 doi:10.20944/preprints202509.1471.v1

Article

Optimal Reaching Method for Enhanced Higher-Order Sliding Mode Control of Electro-Hydraulic Servo Systems

Peng Wan [1], Yunfei Wang [2,*] and Jiawen Yang [1]

[1] Department of Basic Disciplines, Chuzhou Polytechnic College, Chuzhou, 23900, China

[2] School of Safety Engineering, China University of Mining and Technology, Xuzhou, 221116, China

* Correspondence: yunfeiwang@cumt.edu.cn

Abstract

To enhance the position tracking accuracy of heavy-duty asymmetric cylinder electro-hydraulic servo systems subject to unknown matched disturbances, a high-order sliding mode controller with optimal reaching method is proposed, which addresses the robust extension of the classic optimal control problem, which minimizes convergence time under bounded disturbances and system constraints. First, a state-space model of the asymmetric cylinder electro-hydraulic system is established to account for system uncertainties. Second, sliding mode control theory is employed to construct the auxiliary system (i.e., the sliding manifold), and a third-order sliding mode controller with optimal reaching is formulated. Third, Fatou's Lemma and other theorems are applied to prove that the closed-loop system is globally asymptotically stable under the proposed third-order sliding mode controller with optimal reaching. Finally, a simulation model is built using MATLAB/Simulink. The results demonstrate that, compared with Levant's third-order sliding mode controller and the quasi-continuous third-order sliding mode controller, the tracking accuracy of the proposed third-order sliding mode controller with optimal reaching is improved by 7 and 8 orders of magnitude, respectively; the convergence time is reduced by factors of 16.6 and 10.2, respectively, and chattering is significantly suppressed.

Keywords: asymmetric cylinder; electro-hydraulic system; high-order sliding mode control; optimal reaching

1. Introduction

Electro-hydraulic servo systems employ hydraulic fluid as the working medium to facilitate power, motion, and signal transmission through the regulation of pressure energy, flow rate, and flow direction. These systems are characterized by their simpler architecture, compact dimensions, lightweight construction, rapid response, high power density, and ability to enable direct linear motion—attributes that make them indispensable in high-power, high-precision engineering scenarios. Unlike electromechanical systems, their reliance on incompressible hydraulic fluid enables effective force amplification, a critical advantage in applications requiring heavy-load handling. Consequently, they are widely utilized in diverse domains such as robotic arms [1] (for precise end-effector positioning), aircraft simulators [2] (to replicate realistic motion dynamics), vehicle suspensions [3] (for adaptive vibration damping), aerospace engineering [4] (e.g., in flight control actuation), and transportation systems [5] (such as hydraulic braking), thereby demonstrating significant industrial, economic, and scientific research value.

However, electro-hydraulic servo systems are inherently characterized by strong nonlinearity and high-order nonlinear dynamics, stemming from multiple factors: (1) flow-pressure relationships in servo valves, which exhibit nonlinearity due to spool displacement characteristics; (2) fluid compressibility effects, particularly pronounced in long transmission lines, resulting in time-varying

 doi:10.20944/preprints202509.1471.v1

bulk modulus; (3) frictional forces (e.g., Coulomb and viscous friction) between the cylinder piston and casing, which induce discontinuous nonlinearities; (4) asymmetric dynamics in single-rod cylinders, where unequal effective areas on either side of the piston result in asymmetric flow gains during extension and retraction. Compounding these complexities, the presence of unknown variable load forces—such as external disturbances in robotic arm operations or varying payloads in vehicle systems—further exacerbates the challenge of achieving precise control.

Over the past few decades, numerous control strategies have been developed to tackle these challenges. Backstepping control [6,7] decomposes complex nonlinear systems into simpler subsystems, enabling stepwise stabilization, but it often imposes computational burdens in high-order systems. Adaptive control [8,9] adapts parameters in real time to mitigate uncertainties but may display slow convergence under rapid load variations. Robust control [10,11] ensures stability under bounded disturbances but typically requires conservative gains, degrading dynamic performance. Hybrid approaches, such as PID-fuzzy [12] or PID-neural network combinations, enhance adaptability but struggle to balance tracking accuracy and robustness in highly nonlinear regimes—particularly in asymmetric cylinder systems, where their fixed parameter-tuning mechanisms cannot accommodate rapid changes in asymmetric flow gains and external disturbances.

Sliding mode control theory (SMC), grounded in modern control principles, offers a compelling alternative by defining a sliding mode switching surface—a hyperplane in the state space—to steer the controlled system toward this surface and maintain motion along it. A key advantage of SMC is its invariance property: once the system enters the sliding mode, its dynamics are determined solely by the design of the switching surface, endowing it with robustness against matched disturbances and parametric uncertainties. However, conventional first-order or second-order SMC has critical limitations: the high-frequency switching inherent to its control signal triggers "chattering" in the system states (i.e., rapid, undesired oscillations around the sliding surface), which accelerates mechanical degradation in hydraulic components (e.g., servo valve spools) and degrades tracking precision [13]. Moreover, the absence of systematic research on optimizing the "reaching phase"—the transition from the system's initial state to the switching surface—and the subsequent convergence to steady state limits the utilization of SMC's potential in rapid-response scenarios, where minimization of settling time is paramount.

To address these gaps, this paper presents and assesses a high-order sliding mode controller incorporating an optimal reaching law for asymmetric cylinder electro-hydraulic servo systems. Third-order SMC extends conventional low-order configurations by incorporating higher-order derivatives of the tracking error into the sliding surface, which inherently alleviates chattering by smoothing the control signal (through continuous higher-order switching). This design is particularly well-suited for electro-hydraulic systems, where chattering mitigation is critical to prolonging component lifespan.

Two key challenges associated with this control strategy are addressed:

1. Formulating an auxiliary system for the uncertain plant: This system is formulated to encompass the essential dynamics of the asymmetric cylinder, integrating the output variable (e.g., piston displacement) and its first, second, and third time derivatives. By mapping the original system's nonlinearities and uncertainties into this auxiliary framework, the design of the sliding surface and reaching law is simplified.
2. Ensuring optimal performance by solving the "robust Fuller problem": The Fuller problem, a classic optimal control problem, aims to minimize the time to reach a target state under control constraints. Here, it is extended to a "robust" variant by accounting for the auxiliary system's constraints and initial conditions [14], thereby ensuring the reaching phase is both rapid and stable despite parametric uncertainties and external disturbances.

The remainder of this paper is structured as follows: Section 2 presents the mathematical model for asymmetric cylinder electro-hydraulic systems, elaborating on the derivation of state-space

 doi:10.20944/preprints202509.1471.v1

equations from first principles (including valve dynamics, cylinder flow continuity, and force balance). Section 3 presents the "Robust Fuller Problem" in the context of third-order SMC, presents the solution methodology, and delineates the controller design process with stability guarantees. Section 4 assesses and compares position tracking performance between the proposed controller, Levant's third-order SMC [29], and quasi-continuous third-order SMC [30] through simulation. Metrics such as root-mean-square (RMS) tracking error, settling time, and chattering amplitude (quantified by control signal variance) are analyzed to validate the superiority of the optimal reaching strategy. Section 5 summarizes the study with a succinct overview of key findings, limitations, and future research directions (e.g., experimental validation on a physical testbed and extension to multi-axis electro-hydraulic systems).

2. Problem Formulation

The schematic of the valve-controlled asymmetric cylinder position servo system is shown in Figure 1. The hydraulic pressure in the rodless chamber, hydraulic pressure in the rod chamber and output displacement y are measured by sensors and fed back to the controller. The controller adjusts the displacement of the servo valve's main spool to alter the trajectory of the load with mass m, in order to follow the desired trajectory as accurately as possible.

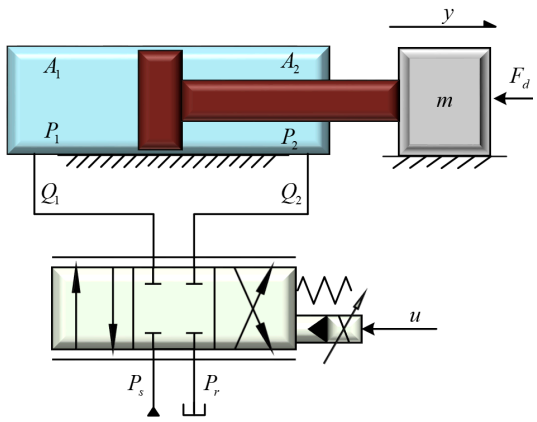

Figure 1. Schematic of the asymmetric cylinder system.

The mechanical equations for the asymmetric cylinder is

$$\mathrm{m}\ddot{y} = (\mathrm{P_1A_1} - \mathrm{P_2A_2}) - \mathrm{b}\dot{y} - \mathrm{F_1} + \mathrm{F_d} \tag{1}$$

where A_1 and A_2 are the effective areas of the rodless and rodded chambers of the asymmetric cylinder, respectively; b is the viscous damping coefficient; F_1 is the external loading force; and F_d is the modeling error (including parameters uncertainties, unmodeled friction, among others).

The flow equation of the proportional servo valve is

$$\begin{cases} \mathrm{Q_1} = \mathrm{k_q x_v}\sqrt{\frac{\mathrm{P_s}}{2} + \mathrm{sgn(x_v)}(\frac{\mathrm{P_s}}{2} - \mathrm{P_1})} \\ \mathrm{Q_2} = \mathrm{k_q x_v}\sqrt{\frac{\mathrm{P_s}}{2} + \mathrm{sgn(x_v)}(\mathrm{P_2} - \frac{\mathrm{P_s}}{2})} \end{cases} \tag{2}$$

where Q_1 and Q_2 are the flow rates of the rodless and rodded chambers of the asymmetric cylinder, respectively; k_q is the flow gain of the proportional servo valve; x_v is the main spool displacement of the proportional servo valve; and P_s is the system supply pressure. Herein, the signum function $sgn(n)$ can be further expressed as

$$\mathrm{sgn(n)} = \begin{cases} 1, & \mathrm{n} > 0 \\ 0, & \mathrm{n} = 0 \\ -1, & \mathrm{n} < 0 \end{cases} \tag{3}$$

Since the response frequency of the proportional servo valve is much higher than that of the entire electro-hydraulic servo system, the main spool displacement of the proportional servo valve is approximated as a first-order proportional relationship with the controller's input voltage, which can

 doi:10.20944/preprints202509.1471.v1

be expressed as $x_v = k_v \cdot u$ .where k_v is the displacement-to-voltage gain coefficient of the proportional servo valve's main spool.

As sealing technology advances, the external leakage coefficient can usually be neglected in the modeling process[15–23]; thus, the flow continuity equation for the asymmetric cylinder is

$$\begin{cases} \dot{P}_1 = \frac{\beta_e}{V_{01}+A_1 y}[Q_1 - A_1\dot{y} - C_t(P_1 - P_2)] + Q_{e1} \\ \dot{P}_2 = \frac{\beta_e}{V_{02}-A_2 y}[-Q_2 + A_2\dot{y} + C_t(P_1 - P_2)] + Q_{e2} \end{cases} \tag{4}$$

where β_e is the bulk modulus of the hydraulic fluid; V_{01} and V_{02} are the initial volumes of the rodless and rodded chambers of the asymmetric cylinder, respectively; C_t is the internal leakage coefficient; and Q_{e1} and Q_{e2} are the modeling errors of the rodless and rodded chambers of the asymmetric cylinder, respectively (including parameter uncertainties, unmodeled dynamics, among others).

Define the system state variable x as

$$x = [x_1, x_2, x_3]^T = [y, \dot{y}, A_1P_1 - A_2P_2]^T \tag{5}$$

The state-space equation of the asymmetric cylinder system can be expressed as

$$\begin{cases} \dot{x_1} = x_2 \\ \dot{x_2} = \frac{1}{m}x_3 - \frac{b}{m}x_2 + d_1 \\ \dot{x_3} = g_1 u - g_2 x_2 - g_3(P_1 - P_2) + d_2 \end{cases} \tag{6}$$

where

$$\begin{cases} R_1 = \sqrt{\frac{P_s}{2} + \mathrm{sgn}(x_v)(\frac{P_s}{2} - P_1)} \\ R_2 = \sqrt{\frac{P_s}{2} + \mathrm{sgn}(x_v)(P_2 - \frac{P_s}{2})} \\ g_1 = (\frac{A_1 R_1}{V_{01}+A_1 y} + \frac{A_2 R_2}{V_{02}-A_2 y})k_t\beta_e \\ g_2 = (\frac{{A_1}^2}{V_{01}+A_1 y} + \frac{{A_2}^2}{V_{02}-A_2 y})\beta_e \\ g_3 = (\frac{A_1}{V_{01}+A_1 y} + \frac{A_2}{V_{02}-A_2 y})\beta_e C_t \\ d_1 = \frac{-F_1+F_d}{2}, d_2 = A_1 Q_{e1} - A_2 Q_{e2}, k_t = k_v \times k_q \end{cases} \tag{7}$$

For the valve-controlled asymmetric cylinder electro-hydraulic position servo system addressed in this paper, the following assumptions are made:

1) The desired trajectory y_d is a continuous,bounded and smooth function, and its first-order derivatives, second-order derivatives, and third-order derivatives exist;

2) The hydraulic pressure in the two chambers of the asymmetric cylinder satisfies $P_r \le P_1, P_2 \le P_s$, where $P_r = 0$.

3. Controller Design

Figure 2 presents the control structure of the proposed method.

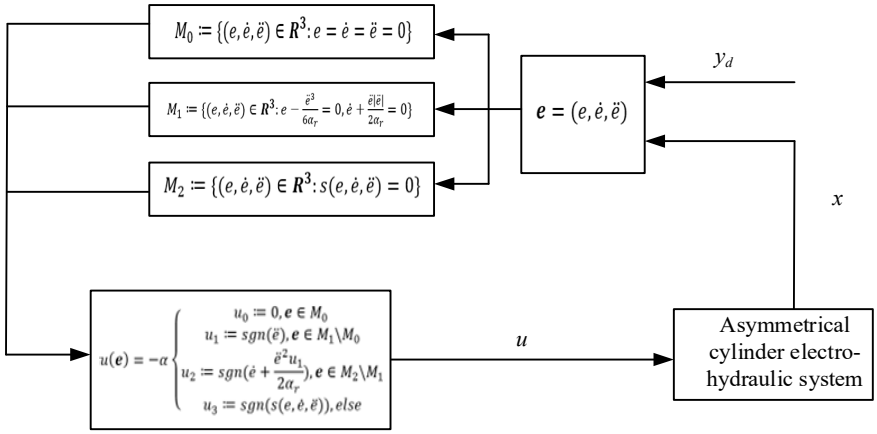

 doi:10.20944/preprints202509.1471.v1

Figure 2. Block diagram of the proposed controller.

Consider the asymmetric cylinder electro-hydraulic system affine with respect to the control variable

$$\begin{cases} \dot{x} = A(x,t) + B(x,t)u(t) \\ y_d(t) = \sigma(x,t) \end{cases} \tag{8}$$

where $x \in R^3$, $\sigma: R^3 \times R \to R$ is a sufficiently smooth objective function. If $A(x,t)$ and $B(x,t)$ are unknown, we refer to (8) is an uncertain system. The order of a sliding mode controller is the minimum order of the time derivatives of the sliding variable $e^{(i)}$ in which the control input u appears.

$$e^{(3)}(t) = \frac{g_1}{m}u + \left(\frac{b^2}{m^2} - \frac{g_2}{m}\right)x_2 - \frac{g_3}{m}P_1 + \frac{g_3}{m}P_2 - \frac{b}{m^2}x_3 + \frac{d_2}{m} - \frac{b}{m}d_1 + \dot{d}_1 + 0.05 * (0.2 * pi)^3 * \cos(0.2 * pi * t) \tag{9}$$

where $e(x,t) = x_1 - \sigma(x,t)$.

Let

$$\begin{cases} h(x,t) := \frac{g_1}{m} \\ g(x,t) := \left(\frac{b^2}{m^2} - \frac{g_2}{m}\right)x_2 - \frac{g_3}{m}P_1 + \frac{g_3}{m}P_2 - \frac{b}{m^2}x_3 + \frac{d_2}{m} - \frac{b}{m}d_1 + \dot{d}_1 + 0.05 * (0.2 * pi)^3 * \cos(0.2 * pi * t) \end{cases} \tag{10}$$

Then

$$e^{(3)}(t) = h(x,t) + g(x,t)u \tag{11}$$

Assume that $h(x,t) \in [-C, C]$ and $g(x,t) \in [K_m, K_M]$, where C, K_m and K_M are positive constants.

The control objective of sliding mode controllers is to reach and maintain the manifold

$$e(x,t) = \dot{e}(x,t) = \ddot{e}(x,t) = 0 \tag{12}$$

in finite time. By introducing

$$\dot{e} = \begin{bmatrix} 0 & 1 & 0 \\ 0 & 0 & 1 \\ 0 & 0 & 0 \end{bmatrix} e + \begin{bmatrix} 0 \\ 0 \\ h(x,t) + g(x,t)u \end{bmatrix} \tag{13}$$

where $e := (e, \dot{e}, \ddot{e})$.

Problem 1(Robust Fuller's Problem)[24]:

$$\begin{cases} \min\limits_{\|v\|_\infty \le \alpha} \max\limits_{\substack{\|h(x,t)\|_\infty \le C \\ K_m \le g(x,t) \le K_M \\ a.e}} \int_0^{+\infty} |e(t)|^v dt \\ \text{Subject to (13) and } e(0) = e_0 \end{cases} \tag{14}$$

The control law for the Robust Fuller's Problem ensures optimality for the worst-case trajectory under matched bounded perturbations. The worst-case trajectory is such that $h(x,t) = -Csgn(u)$ and $g(x,t) = K_m$.

To solve Robust Fuller's Problem, we first introduce Fuller's Problem as follows

Problem 2(Fuller's Problem)[24]:

$$\begin{cases} \min\limits_{\|v\|_\infty \le 1} \int_0^{+\infty} |z_1(t)|^v dt \\ \text{Subject to (13) and } z(0) = z_0 \end{cases} \tag{15}$$

Lemma 1: Assume that $\alpha_r := \alpha K_M - C > 0$. If w^* is an optimal control for Problem 2 with $z_0 = \alpha_r{}^{-1} e_0$, then an optimal control u^* for problem 1 is given by $u^* = \alpha w^*$.

Proof of Lemma 1.

Let

$$z := \alpha_r{}^{-1} e \tag{16}$$

We apply the pontryagin's Maximum Principle[25]. The Hamiltonian function is given

$$H(z, \lambda, h, g, u) = |z_1|^v + \lambda_1 z_2 + \lambda_2 z_3 + \lambda_3 (h + gu) \tag{17}$$

The adjoint system is

$$\begin{cases} \dot{\lambda}_1{}^* = -v|z_1{}^*|^{v-2} z_1{}^* \\ \dot{\lambda}_2{}^* = -\dot{\lambda}_1{}^* \\ \dot{\lambda}_3{}^* = -\dot{\lambda}_2{}^* \end{cases} \tag{18}$$

 doi:10.20944/preprints202509.1471.v1

According to[26], we obtain $\lambda_r^* \neq 0$. Maximization of H with respect to h and g

$$h^* = \mathrm{Csgn}(\lambda_r^*) \tag{19}$$

$$g^* = \begin{cases} K_m, u\lambda_r^* < 0 \\ K_M, u\lambda_r^* > 0 \end{cases} \tag{20}$$

Minimization with respect to u yields $u^* = -\alpha \mathrm{sgn}(\lambda_r^*)$. Thus

$$h^* = -\mathrm{Csgn}(u^*) \tag{21}$$

$$g^* = K_M \tag{22}$$

Let $w := \alpha_r^{-1}(h + gu)$. Then, (13) reduces to

$$\dot{z} = \begin{bmatrix} 1 & 0 & 0 \\ 0 & 1 & 0 \\ 0 & 0 & 1 \end{bmatrix} z + \begin{bmatrix} 0 \\ 0 \\ w \end{bmatrix} \tag{23}$$

Since

$$w^* = \alpha_r^{-1}\left(-\mathrm{Csgn}(u^*) + K_M \alpha \mathrm{sgn}(u^*)\right) = \mathrm{sgn}(u^*) \tag{24}$$

The optimization can be restricted to $\|w^*\|_\infty \leq 1$. Finally

$$u^* = |u^*|\mathrm{sgn}(u^*) = \alpha w^* \tag{25}$$

The solution to Problem 1 has been established in [27]. By using Lemma 1, the solution to the Robust Fuller's Problem is obtained

$$U(e) = -\alpha \begin{cases} u_0 := 0, e \in M_0 \\ u_1 := \mathrm{sgn}(\ddot{e}), e \in M_1 \backslash M_0 \\ u_2 := \mathrm{sgn}(\dot{e} + \frac{\ddot{e}^2 u_1}{2\alpha_r}), e \in M_2 \backslash M_1 \\ u_3 := \mathrm{sgn}(s(e, \dot{e}, \ddot{e})), \text{else} \end{cases} \tag{26}$$

where

$$s(e, \dot{e}, \ddot{e}) := e + \frac{\ddot{e}^3 u_1}{2\alpha_r} + u_2\left[\frac{1}{\sqrt{\alpha_r}}\left(u_2 \dot{e} + \frac{\ddot{e}^2}{2\alpha_r}\right)^{\frac{3}{2}} + \frac{\dot{e}\ddot{e}}{\alpha_r}\right]$$

$$M_0 := \{(e, \dot{e}, \ddot{e}) \in R^3 : e = \dot{e} = \ddot{e} = 0\}$$

$$M_1 := \{(e, \dot{e}, \ddot{e}) \in R^3 : e - \frac{\ddot{e}^3}{6\alpha_r} = 0, \dot{e} + \frac{\ddot{e}|\ddot{e}|}{2\alpha_r} = 0\}$$

$$M_2 := \{(e, \dot{e}, \ddot{e}) \in R^3 : s(e, \dot{e}, \ddot{e}) = 0\}.\square$$

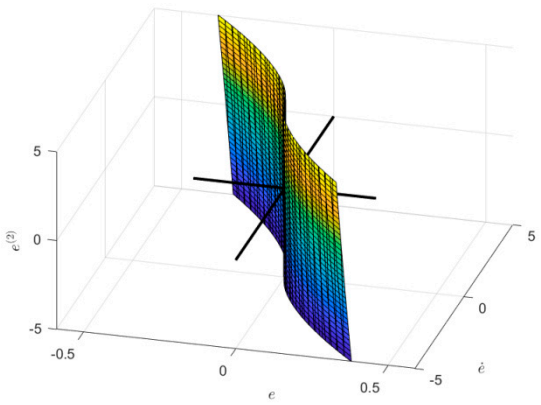

Figure 3. Switching surface.

Theorem 1. Suppose that $\alpha_r > 0$. Then, the origin is a uniformly globally finite-time stable equilibrium of system (13) with control law derived from Problem 1.

Proof of Theorem 1.

For any function $f \in L^\infty$, f_c denotes a function satisfying

$$f_c(t) = f(ct), \text{a. e.} \tag{27}$$

Define a transformation T_c as follows

$$T_c : R^3 \to R^3 \tag{28}$$

 doi:10.20944/preprints202509.1471.v1

$$T_c(x_1, x_2, x_3) = (c^3 x_1, c^2 x_2, c x_3) \tag{29}$$

It is straightforward to verify that

$$e(t; T_{c^{-1}}(e_0), h, g, u) = T_{c^{-1}}\big(e(ct; e_0, h_c, g_c, u_c)\big) \tag{30}$$

Consider the function

$$\begin{cases} V(e_0) := \min\limits_{\|u\|_\infty \le \alpha} \max\limits_{\substack{\|h(x,t)\|_\infty \le C \\ K_m \le g(x,t) \le K_M \\ a.e}} \int_0^{+\infty} |e(t)|^v dt \\ \text{Subject to (13) and } e(0) = e_0 \end{cases} \tag{31}$$

Clearly, we have

$$\begin{cases} V(e_0) \ge 0 \\ V(e_0) = 0 \Leftrightarrow e_0 = 0 \\ V\big(T_c(e_0)\big) = c^{3v+1} V(e_0) \end{cases} \tag{32}$$

These last two properties also imply that V is coercive. Given $\alpha_r > 0$, the system (13) exhibits local finite-time controllability to the origin. Consequently, for any e_0 in a neighborhood of the origin, there exists a control function such that the integral on the right-hand side of the definition of V can be restricted to a finite interval $[0, T]$. Within this interval, e remains bounded, ensuring that V is bounded in a neighborhood of the origin. Recalling that V is homogeneous

$$|V(e_0)| \le c^{-(3v+1)} |V(T_c(e_0))|, \forall c > 0 \tag{33}$$

Since V is bounded in a neighborhood of the origin, the last inequality implies that V is bounded on every compact set.

We now demonstrate that V is lower semi-continuous. Let $e_0^{(k)}$ denote a sequence of initial conditions converging to e_0 and $u^{(k)}, f_1^{(k)}, f_2^{(k)}$ denote a corresponding sequence of optimal solutions. Since V is positive and bounded, we can apply the Fatou's Lemma[28] to obtain

$$\lim\inf_{k\to\infty} \int_0^{+\infty} \left|e(t; e_0^{(k)}, f_1^{(k)}, f_2^{(k)}, u^{(k)})\right|^v dt \ge |V(e_0)|. \tag{34}$$

This confirms lower semi-continuity.

Let

$$L_k := \left\{e \in R^3 : V(e) = \frac{1}{2^k}\right\} \tag{35}$$

$$T_k(e_0, h, g) := \inf\{T : \forall t \ge T, e\big(t; e_0, h, g, U(e)\big) \in L_{k+1}\}. \tag{36}$$

$$\Gamma_k := \sup_{e_0 \in L_k} \sup_{\substack{\|h(x,t)\|_\infty \le C \\ K_m \le g(x,t) \le K_M \\ a.e}} T_k(e_0, h, g) \tag{37}$$

Γ_k is the maximum time required for all the solutions of the differential inclusion (13) reach L_{k+1} when starting from any point in L_k.

Define $c_0 = \frac{1}{2^{3v+1}}$, $e_1 := T_{c_0}(e_0)$, and observe that

$$e_1 \in L_k \Leftrightarrow e_0 \in L_{k+1} \tag{38}$$

$$\begin{aligned} & V\left(e\big(t; e_0, h, g, U(e)\big)\right) \\ &= V\left(T_{c_0}{}^{-1}\big(e\big(c_0 t; e_1, h_{c_0}, g_{c_0}, U(e_{c_0})\big)\big)\right) \\ &= \frac{1}{2} V\left(e\left(c_0 t; e_1, h_{c_0}, g_{c_0}, U(e_{c_0})\right)\right) \end{aligned} \tag{39}$$

Hence

$$T_{k+1}(e_0, h, g) = c_0{}^{-1} T_k(e_1, h, g) \tag{40}$$

By the definition of Γ_k

$$\begin{aligned} \Gamma_{k+1} &= \sup_{e_0 \in L_{k+1}} \sup_{\substack{\|h(x,t)\|_\infty \le C \\ K_m \le g(x,t) \le K_M \\ a.e}} c_0{}^{-1} T_k(e_1, h, g) \\ &= c_0{}^{-1} \sup_{e_1 \in L_k} \sup_{\substack{\|h(x,t)\|_\infty \le C \\ K_m \le g(x,t) \le K_M \\ a.e}} T_k(e_1, h, g) \\ &= c_0{}^{-1} \Gamma_k \end{aligned} \tag{41}$$

Now, we have shown$U(e)$ makes the origin a globally asymptotically stable equilibrium of system (13).□

 doi:10.20944/preprints202509.1471.v1

4. Simulation Results

In this section, simulations are performed using MATLAB/Simulink to validate the effectiveness of the controller proposed in the previous section. Additionally, the proposed third-order sliding mode controller with optimal reaching (OR) is compared with Levant's third-order algorithm (L)[29] and quasi-continuous third-order sliding mode algorithm (QC)[30] to verify the superior performance of the proposed method in an asymmetric cylinder electro-hydraulic system.

The system parameters employed in simulations are summarized in Table 1.

Table 1. Parameters of asymmetric cylinder system.

parameters	value
m/kg	320
P_s/Pa	14*10^6
P_r/Pa	0
b/(N·M)	2000
A_1/m^2	0.0314
A_2/m^2	0.016014
V_{01}/m^3	0.015
V_{02}/m^3	0.008
β_e/Pa	7*10^8
C_t/(m^3·s·Pa)	4*10^{-13}
k_1/(m^3·s·V·Pa$^{1/2}$)	8.91*10^{-8}

The control objective is to regulate the state variable from a specified initial value $x_0 = (x_{10}, x_{20}, x_{30}) = (0,0,0)$ to track a reference trajectory $y_d = 0.05 * \sin(0.2 * pi * t)$, subject to matched disturbances $d_1 = 31.25 * \sin(t)$. Accordingly, a sliding variable e is defined as

$$e = x_1 - 0.05 * \sin(0.2 * pi * t) \tag{42}$$

$$\dot{e} = x_2 - 0.05 * 0.2 * pi * \cos(0.2 * pi * t) \tag{43}$$

$$\ddot{e} = \frac{1}{m}x_3 - \frac{b}{m}x_2 + 0.05 * (0.2 * pi)^2 * \sin(0.2 * pi * t) \tag{44}$$

$$\dddot{e} = \frac{g_1}{m}u + \left(\frac{b^2}{m^2} - \frac{g_2}{m}\right)x_2 - \frac{g_3}{m}P_1 + \frac{g_3}{m}P_2 - \frac{b}{m^2}x_3 + \frac{d_2}{m} - \frac{b}{m}d_1 + \dot{d}_1 + 0.05 * (0.2 * pi)^3 * \cos(0.2 * pi * t)$$
$$= h(x,t) + g(x,t)u \tag{45}$$

Based on the asymmetric cylinder electro-hydraulic system model, the following are derived:

$$h(x,t) \in [-13967, 25362] \tag{46}$$

$$g(x,t) \in [1459.8, 2536] \tag{47}$$

Therefore

$$\dddot{e} \in [-13967, 25362] + [1459.8, 2536]u \tag{48}$$

such that $K_m \approx 1459.8, K_M \approx 2536, C \approx 25362$. To ensure conservatism, $K_m = 1000$, $K_M = 3000, C = 30000$ are set. Thus, a larger bound is adopted as

$$\dddot{e} \in [-30000, 30000] + [1000, 3000]u \tag{49}$$

To satisfy the conditions of lemma 1, $\alpha_r = \alpha K_m - C > 0$ is specified, so that $\alpha > 30$.

Three distinct control laws are denoted as follows: U_L^3 (Levant's third-order slidingmode controller), U_{QC}^3(quasi-continuous third-order sliding mode controller) and U_{OR}^3(third-order sliding mode controller with optimal reaching)

$$U_L^3(e) = -\alpha \mathrm{sgn}[\ddot{e} + \beta_2(|\dot{e}|^3 + e^2)^{\frac{1}{6}} \times \mathrm{sgn}(\dot{e} + \beta_1|e|^{\frac{2}{3}}\mathrm{sgn}(e))] \tag{50}$$

$$U_{QC}^3(e) = -\alpha \frac{(\ddot{e} + \beta_2\left(|\dot{e}| + |e|^{\frac{2}{3}}\right)^{-\frac{1}{2}})(\dot{e} + \beta_1|e|^{\frac{2}{3}}\mathrm{sgn}(e))}{|\ddot{e}| + \beta_2(|\dot{e}| + \beta_1|e|^{\frac{2}{3}})^{-\frac{1}{2}}} \tag{51}$$

$$U_{OR}^3(e) = -\alpha \mathrm{sgn}[e + \frac{\ddot{e}^3}{3\alpha_r^2} + \frac{u_2}{\sqrt{\alpha_r}}\left(u_2\dot{e} + \frac{\ddot{e}^3}{2\alpha_r^2}\right)^{\frac{3}{2}} + \frac{u_2\dot{e}\ddot{e}}{\alpha_r}] \tag{52}$$

 doi:10.20944/preprints202509.1471.v1

$$u_2 \coloneqq \mathrm{sgn}\left(\dot{e} + \frac{\ddot{e}|\ddot{e}|}{2\alpha_r}\right) \tag{53}$$

To ensure a fair comparison, $\alpha = 100$ is fixed, and $\beta_1 = 3$and $\beta_2 = 20$are specified for U_L^3 and U_{QC}^3. For U_{OR}^3, only the control amplitude $\alpha_r = \alpha K_m - C = 70000$ needs to be set.

Simulations are performed over a 0-20s time interval, with results summarized in Figures 4-7: red lines correspond to U_L^3; purple lines to U_{QC}^3; blue lines to U_{OR}^3. Figure 4 presents the output trajectories of all three controllers alongside the reference trajectory

$$y_d = 0.05 * \sin(0.2 * \mathrm{pi} * t).$$

It is observed from Figure 4 that under U_L^3, the system output converges to and tracks the desired trajectory after approximately 0.3s with no significant chattering; under U_{QC}^3, convergence to the target trajectory takes about 0.76s with severe chattering; under U_{OR}^3, the system remains on the target trajectory from the initial state with no noticeable chattering.

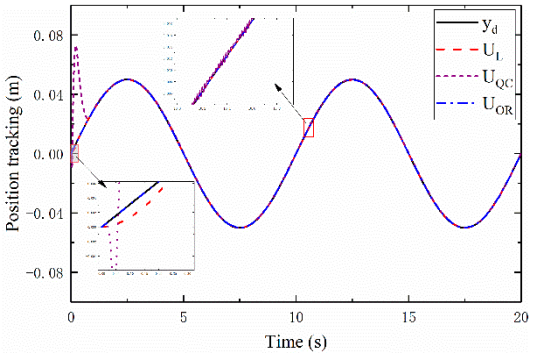

Figure 4. Output Trajectory of different methods.

Figures 5-7, present the time histories of $e, \dot{e}$ and $\ddot{e}$ for the three controllers, respectively. From these figures, U_{OR}^3 exhibits minimal chattering and the smallest average tracking error compared to U_L^3 and U_{QC}^3; the average tracking errors are found to be 3.1667×10^{-5}m、1.4×10^{-3}m and 8.3449×10^{-11}m, respectively. Additionally, in Figure 7, the chattering amplitude of $\ddot{e}$ for U_L^3 is larger than that for U_{OR}^3 and U_{QC}^3, arising from range constraints $[-(C + \alpha K_m), (C + \alpha K_m)]$ imposed by nth-order sliding mode control on the nth derivative of the sliding variable (i.e., $(n-1)$ th derivative of the tracking error)[31].

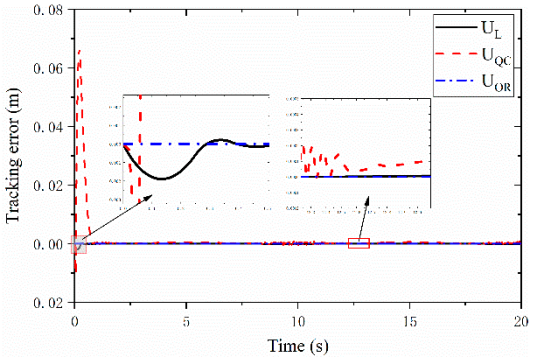

Figure 5. Sliding variable versus time.

 doi:10.20944/preprints202509.1471.v1

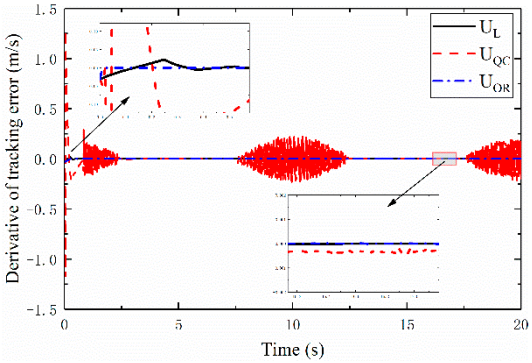

Figure 6. The first order derivative of a sliding variable versus time.

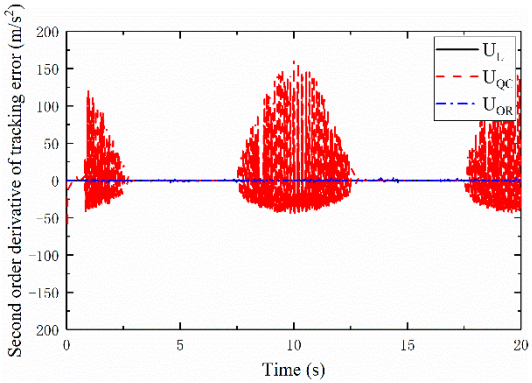

Figure 7. The second order derivative of a sliding variable versus time.

From Figures 4-7, U_{OR}^{3} exhibits advantages over U_{L}^{3} and U_{QC}^{3} in terms of accuracy and convergence time to the reference trajectory. However, the optimal reaching advantage of U_{OR}^{3} is not fully apparent when the initial point lies on the desired trajectory. For a more rigorous comparison, with other parameters unchanged, the reference trajectory is reset to $y_d = 0.05 * \sin(0.2 * pi * t) + 0.02$ and controller activation is delayed by 0.5s.

As shown in Figure 8, U_{L}^{3} takes approximately 1.33s to converge to the reference trajectory from the initial point, U_{QC}^{3} takes about 1.01s, and U_{OR}^{3} takes only 0.55 seconds. Specifically, U_{OR}^{3} converges to the trajectory 0.05 s after activation, which is 16.6 times and 10.2 times faster than U_{L}^{3} and U_{QC}^{3}, respectively.

Figures 9–11 present the time histories of e, $\dot{e}$ and $\ddot{e}$ when tracking$y_d = 0.05 * \sin(0.2 * pi * t) + 0.02$, respectively. The results are consistent with those for $y_d = 0.05 * \sin(0.2 * pi * t)$. The average tracking errors of U_{L}^{3}, U_{QC}^{3} and U_{OR}^{3} after 0.55s are 6.3077×10^{-4}m, 1.3×10^{-3}m and 8.069×10^{-11}m, respectively. From Figures 9-11, the significant advantages of U_{OR}^{3} in accuracy and optimal reaching are fully verified.

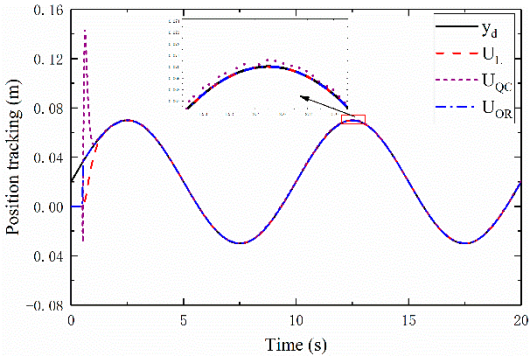

 doi:10.20944/preprints202509.1471.v1

Figure 8. Output Trajectory of different methods.

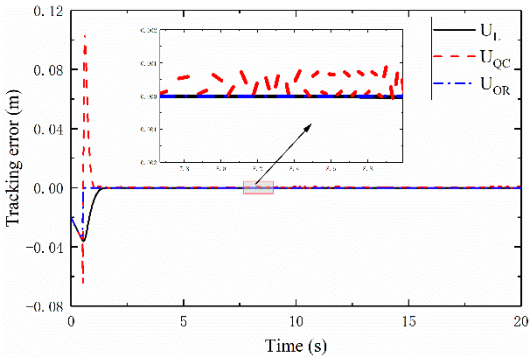

Figure 9. Sliding variable versus time.

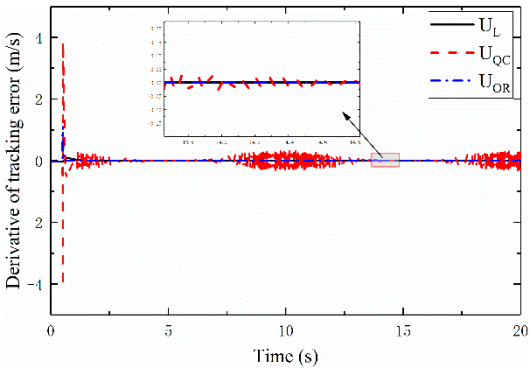

Figure 10. The first order derivative of a sliding variable versus time.

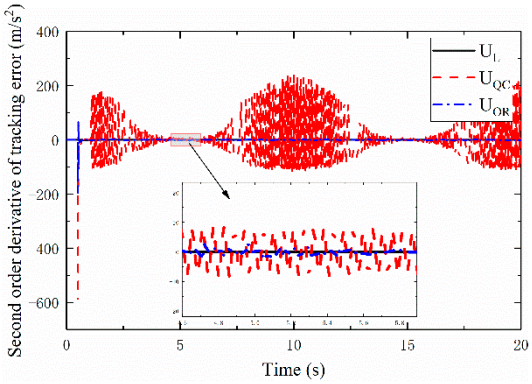

Figure 11. The second order derivative of a sliding variable versus time.

5. Conclusions

1.In this paper, a mathematical model is developed for the asymmetric cylinder electro-hydraulic servo system, and a high-order sliding mode controller is designed for this uncertain system.

2.It is formally proven that the auxiliary system is globally asymptotically stable under the proposed third-order sliding mode controller.

3. A simulation model based on MATLAB/Simulink is constructed, and simulations confirmed that the third-order sliding mode controller exhibited a smaller absolute average tracking error (m). Compared with Levant's third-order sliding mode controller and the quasi-continuous third-order sliding mode controller, the tracking accuracy of the proposed third-order sliding mode controller is

 doi:10.20944/preprints202509.1471.v1

improved by 7 and 8 orders of magnitude, respectively; the convergence time is reduced by factors of 16.6 and 10.2, respectively; and it demonstrates superior chattering suppression capability.

Author Contributions: Theoretical analysis: P.W. and Y.W.; designing experiments and analyzing data: P.W and J.Y.; conducting simulations: P.W. and Y.W.; writing the paper: P.W. ; revising the paper: P.W and J.Y. All authors have read and agreed to the published version of the manuscript.

Funding: This work is supported by the Natural Science Foundation of Jiangsu Province (Grant No. BK20241640) and Scientific Research Project of Anhui Higher Education Institutions (Grant No.2023AH053087).

Data Availability Statement: The datasets generated during and/or analysed during the current study are available from the corresponding author on reasonable request.

Acknowledgments: During the preparation of this manuscript, the authors used MATLAB for the purposes of simulation. The authors have reviewed and edited the output and take full responsibility for the content of this publication.

Conflicts of Interest: The authors declare no conflicts of interest.

Abbreviations

The following abbreviations are used in this manuscript:

OR	Third-order sliding mode controller with optimal reaching
L	Levant's third-order algorithm
QC	Quasi-continuous third-order sliding mode algorithm

References

1. Jing, Baorui. Unknown System Dynamics Estimator for Motion Control of Nonlinear Robotic Systems. *IEEE Transactions on Industrial Electronics* **2020**; *67*: 3850-3859.
2. Han JS. Friction compensation for low velocity control of hydraulic flight motion simulator: a simple adaptive robust approach. *Chinese Journal of Aeronautics* **2013**; *26*: 814-822.
3. Huang Y, Na J, Wu X, et al. Approximation-Free Control for Vehicle Active Suspensions With Hydraulic Actuator. *IEEE Transactions on Industrial Electronics* **2018**; *65*: 7258-7267.
4. Tu JY, Lin PY, Stoten DP, et al. Testing of dynamically substructured, base-isolated system using adaptive control techniques. *Earthquake Engineering & Structural Dynamics* **2009**; *39*: 661-681.
5. Donner R. Emergence of Synchronization in Transportation Networks with Biologically Inspired Decentralized Control. *Springer Berlin Heidelberg* **2009**; *pp*.237-275.
6. Won D, Kim W, Shin D, et al. High-Gain Disturbance Observer-Based Backstepping Control With Output Tracking Error Constraint for Electro-Hydraulic Systems. *IEEE Transactions on Control Systems Technology* **2015**; *23*: 787-795.
7. Guo Q, Zhang Y, Branko G. Celler, et al. Backstepping Control of Electro-Hydraulic System Based on Extended State Observer With Plant Dynamics Largely Unknown. *IEEE Transactions on Industrial Electronics* **2016**; *63*: 6909-6920.
8. Wang C, Quan L, Jiao Z, et al. Nonlinear adaptive control of hydraulic system with observing and compensating mismatching uncertainties. *IEEE Trans. Control Syst. Technol* **2018**; *26*: 927–938.
9. Li X, Yao J, Zhou C. Adaptive robust output-feedback motion control of hydraulic actuators. Int. J. Adapt. *Control Signal Process* **2017**; *31*: 1544–1566.
10. Bakhshande F, Bach R, Sffker D. Robust control of a hydraulic cylinder using an observer-based sliding mode control: Theoretical development and experimental validation-ScienceDirect. *Control Engineering Practice* **2020**; *95*:104272.
11. Shen W, Jiang J, Karimi H R, et al. Observer-Based Robust Control for Hydraulic Velocity Control System. *Mathematical Problems in Engineering* **2013**; 689132.
12. Wang YF, Ding H, Zhao J, et al. Neural network-based output synchronization control for multi-actuator system. *International journal of adaptive control and signal processing* **2022**; *36*: 1155-1171.

 doi:10.20944/preprints202509.1471.v1

13. Utkin V ,Guldner, Jürgen, et al. Sliding Mode Control in Electro-Mechanical Systems, Second Edition. *Crc Press* **2009**; *619*:455-475.
14. G. Bartolini, A. Ferrara, A. Levant, et al. On second order sliding mode controllers. Variable Structure Systems, Sliding Mode and Nonlinear Control, ser. Lecture Notes in Control and Information Series, K. D. Young and U. Ozguner, Eds. London, U.K.: *Springer Verlag* **1999**; *pp*.329–350.
15. Yao B, Al-Majed M. High-performance robust motion control of machine tools: an adaptive robust control approach and comparative experiments. *IEEE/ASME Transactions on Mechatronics* **1997**; *2*: 63-76.
16. Guo K, Wei J, Fang J, et al. Position tracking control of electro-hydraulic single-rod actuator based on an extended disturbance observer. *Mechatronics* **2015**; *27*:47-56.
17. Won D, Kim W, Shin D, et al. High-Gain Disturbance Observer-Based Backstepping Control With Output Tracking Error Constraint for Electro-Hydraulic Systems. *IEEE Transactions on Control Systems Technology* **2015**, *23*: 787-795.
18. Guo Q, Yin JM, Yu T, et al. Coupled-disturbance-observer-based position tracking control for a cascade electro-hydraulic system. *Isa Trans* **2017**; *68*: 367-380.
19. Wang B, Zhang N, Ji H. Study on Precise Displacement Control of a Miniature Hydraulic System via RBF-DOB. *IEEE Access* **2018**, *6*: 69162-69171.
20. Xu ZB, Ma DW, Yao JY. Uniform robust exact differentiator based adaptive robust control for a class of nonlinear systems. *Transactions of the Institute of Measurement and Control* **2018**, *40*: 2901-2911.
21. Guo Q, Li X, Jiang D. Full-state Error Constraints Based Dynamic Surface Control of Electro-hydraulic System. *IEEE Access* **2018**, *PP*. 1-1.
22. JI X hao, WANG Cheng wen, CHEN Shuai, et al. Sliding mode back-stepping control method for valve-controlled electro-hydraulic position servo system[J]. *Journal of Central South University* **2020**, *51*: 1518−1525.
23. Xiong Y, Wei J, Feng R, et al. Disturbance observer based pressure control for electrohydraulic system. *Journal of Central South University* **2017**, *48*: 1182-1189.
24. A.T. Fuller. Relay control systems optimized for various performance criteria. *IFAC Proceedings Volumes* **1961**,*1*: 520-529.
25. Pontrjagin L S. The Mathematical Theory of Optimal Processes. *Interscience* **1962**, *16*: 493-494.
26. G. Bartolini, A. Ferrara, E. Usai and V. I. Utkin. On multi-input chattering-free second-order sliding mode control. *IEEE Transactions on Automatic Control* **2000**, *45*: 1711-1717.
27. A. A. Feldbaum. On synthesis of optimal systems with the help of phase space. *Avtomatika i telemehanika* **1955**, *16*: 129–149.
28. Apelian C, Surace S, Mathew A. Real and Complex Analysis. *McGraw-Hill* **2009**.
29. Levant A. Universal single-input-single-output (SISO) sliding-mode controllers with finite-time convergence. *IEEE Transactions on Automatic Control* **2001**, *46*: 1447-1451.
30. Levant A. Quasi-Continuous High-Order Sliding-Mode Controllers. *IEEE Transactions on Automatic Control* **2005**, *50*: 1812-1816.
31. F. Dinuzzo, A. Ferrara. Higher Order Sliding Mode Controllers With Optimal Reaching. *IEEE Transactions on Automatic Control* **2009**, 54: 2126-2136.